Chemo-mechanical modelling of swelling of cementitious materials subjected to external sulfate attacks

J Pouya, Mejdi Neji, Laurent de Windt, Frédéric Péralès, J Corvisier, A Socie

Chemo-mechanical modelling of swelling of cementitious materials subjected to external sulfate attacks

J. POUYA[a] , M. NEJI[a] , L. DE WINDT[b] , F. PERALES[c] , J. CORVISIER[b] , A. SOCIE[b]

a. Institut de Radioprotection et de Sûreté Nucléaire (IRSN), PSE-ENV/SEDRE/LETIS, Fontenay-aux-Roses, 92260, France
julie.pouya@irsn.fr
mejdi.neji@irsn.fr
frederic.perales@irsn.fr

b. MINES ParisTech, Université PSL, Fontainebleau, France
laurent.dewindt@mines-paristech.fr
jerome.corvisier@mines-paristech.fr
adrien.socie@mines-paristech.fr

Résumé :

Cette étude s'inscrit dans le cadre de l'évaluation de sûreté concernant la durabilité des bétons employés pour la conception et la réalisation d'un stockage de déchets radioactifs en formation géologique profonde. Les bétons peuvent être soumis à des attaques sulfatiques externes modérées, conduisant à la précipitation de gypse et d'ettringite dans le milieu poreux. La formation de ces minéraux engendre des pressions de gonflement interne, conduisant à une fissuration et une expansion du matériau, réduisant ses propriétés de confinement. Cet article présente les résultats expérimentaux obtenus sur des échantillons de pâte de ciment soumis à une attaque sulfatique externe à faible concentration (30.10^{-3} mol/l) pendant 6 mois dans des conditions de service réalistes. Les échantillons ont été caractérisés à l'aide de plusieurs outils de caractérisation expérimentale tels que la DRX, le MEB-EDS et la nanoindentation afin de suivre l'évolution des propriétés chimiques, minéralogiques, microstructurales et mécaniques du matériau. Des échantillons de pâte de ciment avec différents ratios en C_3A ont été utilisés pour favoriser la formation d'ettringite ou de gypse pendant l'attaque chimique afin d'évaluer l'impact de chaque minéral sur la dégradation. Les résultats mettent en évidence l'apparition de fissures parallèles à la surface d'attaque, situées dans la zone de formation de gypse et de dissolution de la portlandite. Cette observation suggère une participation active de la formation de gypse dans le mécanisme d'expansion. Des simulations numériques de la dégradation chimique ont été réalisées en utilisant le code de transport réactif HYTEC afin d'enrichir l'interprétation des résultats expérimentaux. Sur la base des résultats de la simulation, un schéma d'homogénéisation analytique a été appliqué pour estimer les valeurs du module d'Young dans la zone dégradée. Les valeurs de

profondeur des fronts de dégradation et les propriétés élastiques calculées étaient en bon accord avec les résultats expérimentaux.

Mots clefs : Couplage chimio-mécanique, transport réactif, Modèle de Zones Cohésives, pâte de ciment CEM I, homogénéisation.

Abstract:

Durability of concrete exposed to an external sulfate attack is a great concern for long-time reliability of nuclear waste containment. Concrete can be subjected to moderate external sulfate attacks, leading to the precipitation of gypsum and ettringite in the porous media. The formation of these minerals generates internal swelling pressures, leading to cracking and expansion of the material, reducing its containment properties. This paper presents experimental results obtained on cement paste samples subjected to a low concentration (30.10^{3} mol/l) external sulfate attack during 6 months in realistic service conditions. Samples were characterized using multiple experimental characterization tools such as XRD, SEM-EDS, and nanoindentation to follow the evolution of chemical, mineralogical, microstructural and mechanical properties of the material. Cement paste samples with different C_3A ratios were used to boost either ettringite or gypsum formation during the chemical attack in order to assess the impact of each mineral on the degradation. Results showed apparition of cracks parallel to the attacked surface, located in the gypsum formation and portlandite dissolution area. This observation suggested an active participation of gypsum formation in the expansion mechanism. Numerical simulations of the chemical degradation were performed using the reactive transport code HYTEC in order to enrich the interpretation of experimental results. Based on simulation results, an analytical homogenization scheme was applied to estimate Young Modulus values in the degraded area. Depth values of degradation fronts and calculated elastic properties were in good agreement with experimental results.

Keywords : Chemo-mechanical coupling, reactive transport, Cohesive Zone Model, CEM I cement paste, homogenization.

1   Introduction

This study assesses the containment durability of cementitious materials in the context of deep geological nuclear waste repositories. Concrete would be used as a buffer material located around steel waste packages or as a mechanical support of sealing systems. The geological groundwater, in contact with waste packages or sealings, contains sulfate ions in low concentrations which may diffuse in the concrete porous media, leading to external weak sulfate attacks [1,2]. Low concentration sulfate attacks are characterized by the precipitation of secondary ettringite and gypsum that affects chemical and microstructural properties. A significant precipitation of these minerals in the porous media eventually leads to swelling pressure and ultimately to cracking, macroscopic expansion, spalling and loss of strength of the material [3,4]. Thus, external sulfate attacks are widely known as a real threat to concrete durability. However, the reaction phenomenology still raises questions. The processes involved result from the coupling between chemical reactions, diffusive transport and mechanical response of the material [5]. Furthermore, even though the damaging impact of ettringite formation is well established, great expansion for materials with low C_3A content has been observed due to significant gypsum formation [6], suggesting that gypsum precipitation should also be taken into consideration as a factor

of expansion. However, the exact mechanism of the impact of gypsum formation on expansion remains unclear. Another relevant process that may occur during external sulfate attacks is hydrolysis by sulfate solutions with pH lower than 12. Calcium leaching resulting from portlandite dissolution and C-S-H decalcification contribute to the weakening of the material and should be considered as a consequence of external sulfate attacks [7]. However, the contribution of expansive product precipitation and calcium leaching on the material damage is difficult to properly quantify. In order to assess the phenomenology involved during such degradation processes under realistic disposal conditions, the coupled chemo-mechanical evolution of CEM I cement pastes was studied by combining mineralogical and mechanical analyses with reactive transport and mechanical modeling.

2   Materials and modeling
2.1   Experimental setup

The present study is designed to provide data about the degradation mechanism of cement pastes subjected to external sulfate attacks in order to understand both the impact of gypsum and ettringite formation, and decalcification on material damage. The experimental setup consisted of the immersion of CEM I hydrated cement pastes (w/c = 0.5) in a low-concentration sodium sulfate solution (30 mmol/L), representative of naturally occurring conditions. Samples were extracted for analysis at specific timeframes ranging from 15 days to 6 months. The samples were initially protected from lateral degradation by an epoxy coating to allow a unidirectional sulfate attack. C_3A-rich and C_3A-poor cement formulations were used to boost, respectively, ettringite or gypsum formation during the chemical attack. The objective is to compare the degradation of a cement paste with variable quantities of ettringite and gypsum to discriminate the effect of each mineral on the material damage. Various mineralogical and mechanical characterization methods were used in order to assess the phenomenology of the degradation mechanism:

- Chemical and microstructural changes of samples were investigated by SEM-EDS analyses.
- XRD analyses provided data about mineralogical evolution with depth.
- Nanoindentation acquisition was performed to determine mechanical properties evolution of leached pastes.

Measurements were done at the microstructure scale of the cement paste to identify the microstructure evolution taking place during the degradation.

2.2   Modeling approach

To support the interpretation of experimental results, reactive transport modeling of both cement pastes subjected to a weak external sulfate attack was performed with the HYTEC code [8] using Thermoddem thermodynamic database [9]. Simulations considered a variable porosity. The initial effective diffusion coefficient was fitted to the experimental degradation front of the C_3A-rich cement paste after 4 months. The initial mineralogical compositions were determined from the bulk chemistry and XRD data. Both hydrated cement pastes contained portlandite, C-S-H, ettringite and monocarboaluminate, but in different proportions. The chemical degradation of the matrix phases, C-S-H, was introduced with a decreasing Ca/Si ratio from 1.6 to 0.7 to properly model their progressive decalcification. The model considers the full aqueous chemistry (acid/base, complexation). The mechanical properties of the degraded zones were estimated by an analytical homogenization scheme, the Mori-Tanaka scheme, based on the calculated mineral volume fractions and porosity, considering the hardened cement paste as a series of inclusions embedded in an infinite matrix.

3   Results

3.1   Microstructural and mineralogical evolution of CEM I pastes exposed to external sulfate attacks

Figure 1 displays the calculated mineral volume fractions and total porosity (capillary porosity and gel porosity) plotted as a function of depth and compared to intensity ratios of calcium and sulfur extracted from SEM-EDS analysis for C_3A rich and poor samples. For both pastes, simulation results showed a first front of monocarboaluminate and partial portlandite dissolution, combined to secondary ettringite precipitation, induced by the diffusion of sulfates. A second front occurred closer to the exposed surface, consisting of gypsum formation associated with massive portlandite dissolution. Formation of C-S-H with a decreasing Ca/Si ratio from 1.6 to 0.8 is showed from the sound core to the exposed surface. Regarding experimental results, a decrease of the intensity ratio of calcium was detected in the degraded area. A sulfur-enriched zone was identified for both pastes, corresponding to gypsum formation according to XRD acquisition results.

However, differences were noticed between the C_3A-rich and the C_3A-poor samples. First, in case of the C_3A-poor cement paste, the simulated gypsum precipitation front was located where the experimental sulfur-enriched zone was detected. The calculated gypsum precipitation thickness was in line with experimental measurements, but slightly underestimated. However, in case of the C_3A-rich cement paste, the calculated gypsum formation thickness was smaller than the experimental one. Furthermore, apparition of cracks located in the calcium depleted area and parallel to the attacked surface was observed for the degraded C_3A-rich paste. Cracks occurred in a zone where secondary ettringite and a high amount of gypsum were detected, probably induced by swelling due to these mineral precipitations. The thickness of the main crack was about 300 µm. This great opening can be attributed to the large amount of gypsum that precipitated after 6 months of immersion in the sodium sulfate solution.

The evolution of mineralogical composition and microstructural properties was globally well captured by the reactive transport model, such as a higher quantity of gypsum and lower formation of ettringite in the C_3A-poor sample. The evolution of the calculated chemical front depths as a function of time was also in good agreement with experimental results, except in the case of the C_3A-rich paste after 6 months of degradation. The experimental calcium-depleted zone was 1000 µm larger for the C_3A-rich paste, suggesting a crack effect in the observed degradation. This effect was not considered in the presented HYTEC simulations. Finally, in line with the experimental data, modeling led to a gradual increase of total porosity due to the total dissolution of portlandite and the progressive decrease of Ca/Si ratio of C-S-H.
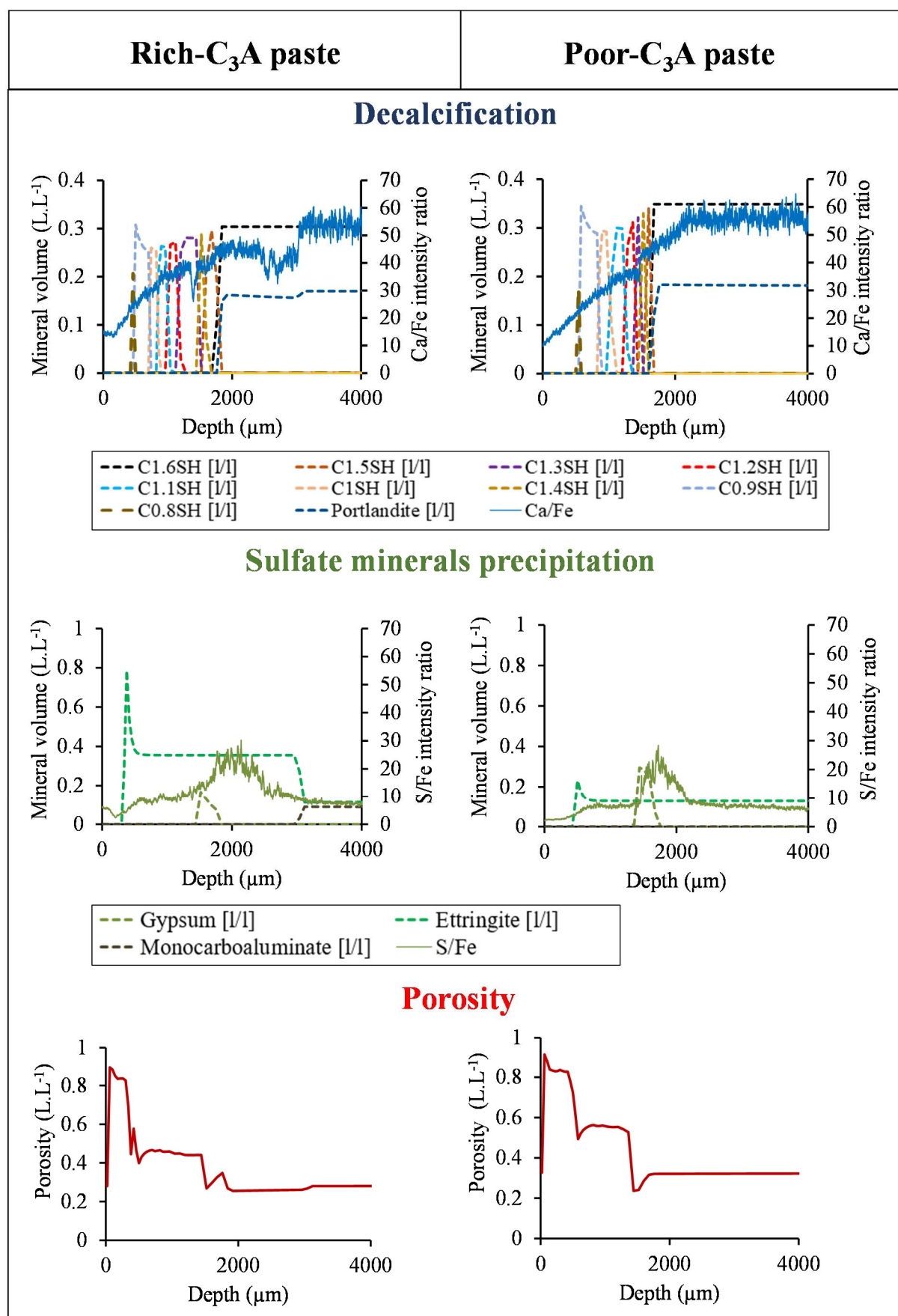
Figure 1. Profiles of minerals and porosity obtained at 180 days (HYTEC simulation) and Ca/Fe and S/Fe intensity ratio built from EDS map after 6 months in the 30.10^{-3} mol.L^{-1} Na_2SO_4 solution at pH 7.

3.2   Characterization   of   the   mechanical   properties   by nanoindentation and homogenization methods

Nanoindentation measurements were performed on each sample going from one exposed surface to the other. Average properties values were calculated at each measured depth. Results showed a decrease of the elastic modulus from the center of the paste to the attacked surface, over a depth of 2000 µm for the C_3A-poor sample and 3000 µm for the C_3A-rich sample (figure 2). In the case of the C_3A-poor sample, the curve displaying the average of the elastic modulus measured as a function of depth indicated a linear decrease in the leached zone, from 20 GPa to 5 GPa. Similarly, results showed that the measured Young moduli decreased as the intensity ratio of calcium dropped, which suggested a loss of mechanical properties given by the decalcification of the sample. Regarding the C_3A-rich cement paste, a similar decrease of Young moduli going from 20 GPa to less than 5 GPa near the exposed surface was also observed, correlated to the reduction of the calcium intensity ratio. A sharp drop of elastic properties was detected in the cracked areas.

The micro-mechanical properties were then calculated from the chemical HYTEC modeling results and compared to the experimental data. The local mechanical properties associated with the precipitation and dissolution of minerals are estimated by analytical homogenization methods from the total porosity and volume fractions of minerals. The Mori-Tanaka homogenization scheme [10] was used, considering a cement paste whose matrix is composed of C-S-H (comprising one or more families distinguished by the Ca/Si ratio) and inclusions randomly distributed in orientation and space. The inclusions in the scheme are hydrates, anhydrous cement, capillary porosity. The total porosity ϕ includes two families of pores, gel pores and capillary pores, respectively noted ϕ_{C-S-H} and ϕ_{cap} in the following equation:

$$\phi = \phi_{C-S-H} + \phi_{cap} \tag{1}$$

Based on Tennis and Jenning work [11], gel porosity is estimated from C-S-H volume fraction:

$$\phi_{C-S-H} = \alpha_{C-S-H} \; \varphi_{C-S-H} \tag{2}$$

where α_{C-S-H} is a coefficient equal to 0.35 [12], and φ_i the volume fraction of phase i.
At the cement paste scale, the following equation must be satisfied:

$$1 = \phi_{cap} + \sum_{i}^{Nph} \varphi_i \tag{3}$$

where Nph is the number of phases.
C-S-H equivalent volume fraction and capillary porosity were estimated from the previous equations and given respectively by equations 4 and 5:

$$\phi_{cap} = \frac{\phi - \alpha_{C-S-H} \left(1 - \sum_{i}^{Nph-1} \varphi_i + \varphi_{C-S-H}\right)}{1 - \alpha_{C-S-H}} \tag{4}$$

$$\varphi_{C-S-H} = \frac{\left(1 - \sum_{i}^{Nph-1} \varphi_i\right) - \phi)}{1 - \alpha_{C-S-H}} \tag{5}$$

The homogenization method was applied based on the volume fractions of each mineral phase provided by the previous chemical degradation simulations. The mechanical properties of minerals were taken from Haecker et al. [13]. Determination of C-S-H mechanical properties were based on Constantinides and Ulm work [14]. They estimated the elastic modulus of sound and degraded C-S-H as 23.8 and 4.3 GPa, respectively. Subsequently, these values were used to determine the evolution of the decalcified C-S-H Young modulus E_{CSH} as a function of their Ca/Si (noted C/S) ratio, based on the following equation [15]:

$$\begin{cases} if \quad \dfrac{C}{S} > 0.8, \quad E_{CSH} = \left(1 - \dfrac{C/S - 0.8}{1.65 - 0.8}\right) E_{CSH}^{UL} + \dfrac{C/S - 0.8}{1.65 - 0.8} E_{CSH}^{S} \\ if \quad \dfrac{C}{S} \leq 0.8, \quad\quad\quad\quad\quad\quad\quad\quad E_{CSH} = E_{CSH}^{UL} \end{cases} \tag{8}$$

where E_{CSH}^{UL} and E_{CSH}^{S} are Young modulus of leached and sound C-S-H, respectively.

Poisson ratio values were assumed to be unaffected by calcium leaching, as well as the volume fractions of the two types of C-S-H [15].

A slight decrease of the Young modulus (Figure 2) was observed on both C$_3$A-rich and C$_3$A-poor cement pastes at the monocarboaluminate and ettringite transformation front linked to the partial dissolution of portlandite (Figure 1). A more significant decrease occurred at total dissolution front of the portlandite. This change took place in several stages, corresponding to the various C-S-H decalcification fronts. In the most decalcified zone, where the ettringite was completely dissolved and only amorphous gel remained, the Young modulus attained its final value of 5 GPa for both types of cement pastes, in good agreement with the experimental results.

Nevertheless, differences were observed between the two types of cement pastes. The Young modulus quickly reached values lower than 10 GPa in the C$_3$A-poor paste after the decrease related to the total dissolution of portlandite. In the case of the C$_3$A-rich paste this mechanical property varied between 15 GPa and slightly below 10 GPa over the whole zone not entirely decalcified. These two modeling results were in good agreement with experimental measurements, since the mechanical properties measured in the C$_3$A-rich paste, at the level of the non-cracked zones, attained higher values than in the case of the C$_3$A-poor paste. Since cracking was not considered in the chemical simulations, the rapid decrease in mechanical properties measured experimentally due to the presence of cracks could not be represented in the homogenization results.
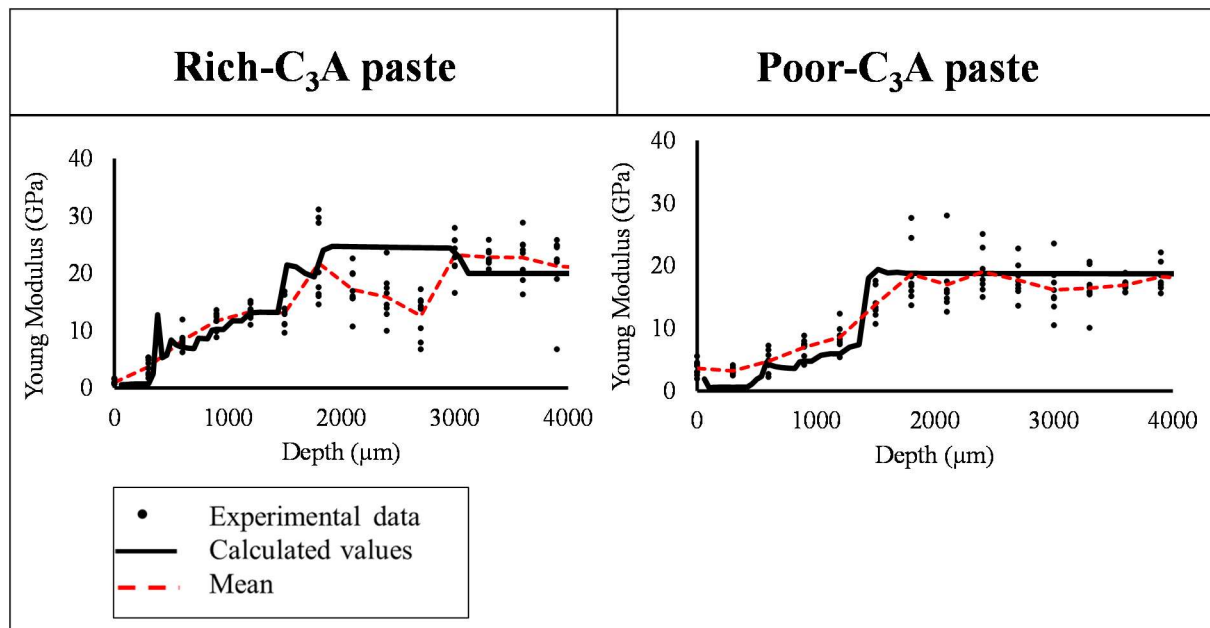
Figure 2. Evolution of discrete Young modulus and mean values with depth obtained by nanoindentation, compared to the calculated elastic properties obtained by the homogenization method based on HYTEC modeling results.

4   Conclusion and perspectives

Experimental results were obtained on cement pastes subjected to a low concentration external sulfate attack under realistic disposal conditions. The multiple-techniques approach (XRD, SEM-EDS and nanoindentation) led to an accurate characterization of the coupled evolution of chemical, mineralogical, microstructural and mechanical properties. A significant result was the occurrence of cracks parallel to the exposed surface, located in the gypsum formation zone, showing the potential effect of gypsum precipitation on the generation of swelling pressure and cracking. Reactive transport modeling combined to an analytical homogenization technique supported the interpretation of experimental results by investigating the effect of both sulfate products formation and mineral leaching on sample resistance. Nevertheless, the model failed to simulate the acceleration of the degradation by crack formation. Therefore, in order to study the cracking of the material by considering the diffusion of species in the cracks, chemo-mechanical simulations will be performed with the numerical platform XPER [15]. The chemo-mechanical model is based on the coupling between reactive transport and a poromechanical model in a cracked heterogeneous porous medium. Work is in progress to simulate the crack initiation by chemical expansion as well as the effect of the cracks on the reactive transport kinetics.

References

[1] Figg, J. Field studies of sulfate attack on concrete. American Ceramic Society, Inc, Materials Science of Concrete: Sulfate Attack Mechanisms (USA), 1999, 315–323.

[2] Tulliani, J.-M., Montanaro, L., Negro, A., Collepardi, M. Sulfate attack of concrete building foundations induced by sewage waters. Cement and Concrete Research 32, 2002, 843–849.

[3] Ragoug, R., Metalssi, O.O., Barberon, F., Torrenti, J.-M., Roussel, N., Divet, L., de Lacaillerie, J.-B. d'Espinose. Durability of cement pastes exposed to external sulfate attack and leaching: Physical and chemical aspects. Cement and Concrete Research 116, 2019, 134–145.

[4] Yu, C., Sun, W., Scrivener, K. Mechanism of expansion of mortars immersed in sodium sulfate solutions. Cement and concrete research 43, 2013, 105–111.

[5] Le Bescop, P., Solet, C. External sulphate attack by ground water: Experimental study on CEM I cement pastes. Revue européenne de génie civil 10, 2006, 1127–1145.

[6] Gonzalez, M.A., Irassar, E.F. Ettringite formation in low C3A Portland cement exposed to sodium sulfate solution. Cement and Concrete Research 27, 1997, 1061–1071.

[7] Qin, S., Zou, D., Liu, T., Jivkov, A. A chemo-transport-damage model for concrete under external sulfate attack. Cement and Concrete Research 132, 2020, 106048.

[8] Van Der Lee, J., De Windt, L., Lagneau, V., Goblet, P., 2003. Module-oriented modeling of reactive transport with HYTEC. Computers & Geosciences 29, 265–275.

[9] Blanc, P., Lassin, A., Piantone, P., Azaroual, M., Jacquemet, N., Fabbri, A., Gaucher, E.C. Thermoddem: A geochemical database focused on low temperature water/rock interactions and waste materials. Applied Geochemistry 27, 2012, 2107–2116.

[10] Mori, T., Tanaka, K. Average stress in matrix and average elastic energy of materials with misfitting inclusions. Acta metallurgica 21, 1973, 571–574.

[11] Jennings, H.M., Tennis, P.D. Model for the developing microstructure in Portland cement pastes. Journal of the American Ceramic Society 77, 1994, 3161–3172.

[12] Bahafid, S., Ghabezloo, S., Duc, M., Faure, P., Sulem, J. Effect of the hydration temperature on the microstructure of Class G cement: CSH composition and density. Cement and Concrete Research 95, 2017, 270–281.

[13] Haecker, C.-J., Garboczi, E.J., Bullard, J.W., Bohn, R.B., Sun, Z., Shah, S.P., Voigt, T. Modeling the linear elastic properties of Portland cement paste. Cement and Concrete Research 35, 2005, 1948–1960.

[14] Constantinides, G., Ulm, F.-J. The effect of two types of CSH on the elasticity of cement-based materials: Results from nanoindentation and micromechanical modeling. Cement and concrete research 34, 2004, 67–80.

[15] Stora, E., Bary, B., He, Q.-C., Deville, E., Montarnal, P. Modelling and simulations of the chemo–mechanical behaviour of leached cement-based materials: leaching process and induced loss of stiffness. Cement and Concrete Research 39, 2009, 763–772.

[16] Perales, F., Dubois, F., Monerie, Y., Piar, B., Stainier, L. A nonsmooth contact dynamics-based multi-domain solver: code coupling (Xper) and application to fracture. European Journal of Computational Mechanics/Revue Européenne de Mécanique Numérique 19, 2010, 389–417.